



## ARTICLE

# Thiazolidine-4-one clubbed pyrazoles hybrids: Potent $\alpha$ -amylase and $\alpha$ -glucosidase inhibitors with NLO properties

Parvin Kumar<sup>1</sup> | Meenakshi Duhan<sup>1</sup> | Jayant Sindhu<sup>2</sup> | Kulbir Kadyan<sup>1</sup> | Sangeeta Saini<sup>1</sup> | Neeraj Panihar<sup>3</sup>

<sup>1</sup>Department of Chemistry, Kurukshetra University, Kurukshetra, India

<sup>2</sup>Department of Chemistry, COBS&H CCS Haryana Agricultural University, Hisar, India

<sup>3</sup>Department of Pharmaceutical Science, G.J.U.S.T, Hisar, India

## Correspondence

Parvin Kumara, Department of Chemistry, Kurukshetra University, Kurukshetra 136119, India.  
Email: parvinchem@kuk.ac.in; parvinjangra@gmail.com

## Abstract

Molecular hybrids based on thiazolidin-4-one and pyrazolyl pharmacophore (THZP) as new antidiabetic agents were synthesized. Two sets of signals came into view in <sup>1</sup>H NMR of THZP8-THZP14 exhibited the presence of a configurational isomeric mixture of 2*E*,5*Z* (38.24%-41.58%) and 2*Z*,5*Z* isomers (58.42%-61.76%), which was further endorsed by density functional theory (DFT) studies. All the compounds exhibit promising nonlinear optical properties (NLO). Further, the biological potential of THZPs was explored in terms of  $\alpha$ -amylase and  $\alpha$ -glucosidase inhibition. DFT-based descriptors were calculated to describe the reactivity, and a relationship was developed with biological activities. THZP9 and THZP14 showed remarkable inhibition of  $\alpha$ -amylase and  $\alpha$ -glucosidase with IC<sub>50</sub> 9.90  $\mu$ M and 4.84  $\mu$ M, respectively, as compared with standard drug acarbose.

## 1 | INTRODUCTION

Medicinal chemists are putting serious efforts to control diabetes-related mortality; nevertheless, this disease is still alarming and also increasing each year.<sup>[1-3]</sup> The life sustainability of hyperglycemic patients depend extensively on blood glucose level and thus regulating its level can be considered as a real challenge in the scientific arena.<sup>[4]</sup> The prolonged hyperglycemic condition is a prime mortality factor that partially results from its effect on structural and functional aspect of vital proteins.<sup>[5]</sup> It is presumed that hyperglycemia enhances the creation of free radicals and reactive oxygen species leading to oxidative tissue damage, which further leads to various complications such as neuropathy,<sup>[6,7]</sup> nephropathy,<sup>[8,9]</sup> retinopathy,<sup>[10,11]</sup> and cardiovascular disorders.<sup>[12,13]</sup>

The postprandial hyperglycemic condition in patients with diabetes is because of hydrolysis of dietary carbohydrates, which is governed by two enzymes, ie,  $\alpha$ -glucosidase and  $\alpha$ -amylase.<sup>[14,15]</sup> Suspension of glucose

absorption after a meal by inhibiting these two enzymes is an influential method for the alleviation and treatment of type 2 diabetes mellitus (T2DM). Furthermore, the complications of modified immune responses and metabolic disorders can be controlled by regulating the activity of  $\alpha$ -amylase and  $\alpha$ -glucosidase.<sup>[16]</sup> Currently, voglibose and acarbose are frequently used as  $\alpha$ -glucosidase and  $\alpha$ -amylase inhibitors to control postprandial hyperglycemic condition.<sup>[17]</sup> The effectiveness of these drugs for the treatment of T2DM is repressed due to various side effects such as flatulence, abdominal distension, and diarrhoea associated with their exposure.<sup>[18]</sup> The side effects associated with marketed drugs is a significant mode to devise novel inhibitors that are more effective and safer for the treatment of T2DM.<sup>[19,20]</sup>

Thiazolidine-4-one, a privileged pharmacophore, came into existence for its role as an antihyperglycemic agent and is a part of a number of antidiabetic drugs.<sup>[21,22]</sup> Thiazolidin-4-one has been emerged as a very persuasive scaffold because of its clinical significance and

widespread pharmacological activities associated with it.<sup>[23–30]</sup> Similarly, another significant class of compound, named pyrazole has a broad range of biological activities such as anti-inflammatory, antifungal,<sup>[31]</sup> antioxidant,<sup>[32]</sup> antitumor,<sup>[33]</sup> antihypertensive, antibacterial,<sup>[34]</sup> anticancer activity,<sup>[35]</sup> and antidiabetic activities<sup>[36]</sup> associated with it.

Persisting our interest in the design and development of biologically active heterocyclic compounds<sup>[22,24,37–41]</sup> and novel inhibitor of  $\alpha$ -amylase<sup>[22]</sup> we, herein, report the design and synthesis of a hybrid scaffold having thiazolidin-4-one and pyrazole in a single matrix. <sup>1</sup>H NMR and density functional theory (DFT) studies explored the isomerization in the synthesized compounds. All the newly synthesized molecular hybrids were screened in vitro for their inhibitory potential against  $\alpha$ -amylase and  $\alpha$ -glucosidase. The docking study of the most active compound was performed to investigate the interaction with the binding site of  $\alpha$ -amylase and  $\alpha$ -glucosidase.

## 2 | RESULT AND DISCUSSION

### 2.1 | Chemistry

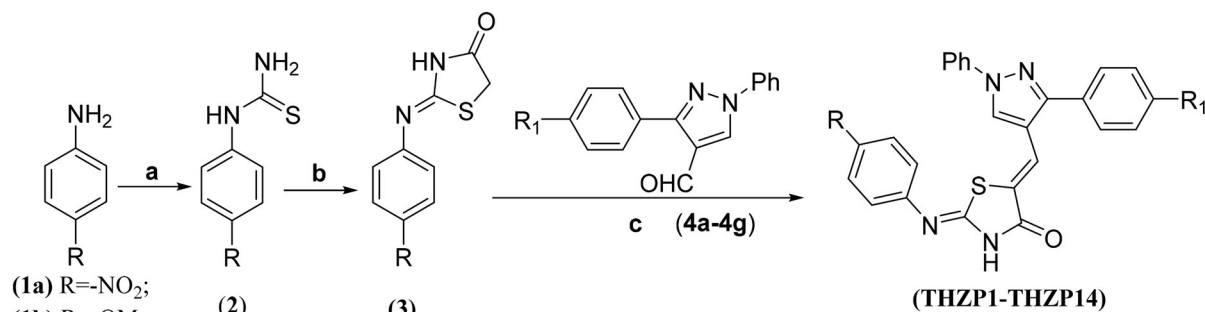
The following synthetic methodology achieved the synthesis of molecular hybrids (**THZP1-THZP14**) based on thiazolidine-4-one and pyrazole. The key reactant 2-(*p*-arylimino)thiazolidin-4-one (**3**), required for the synthesis of molecular hybrids (**THZP1-THZP14**), was prepared by condensing 4-substituted arylthiourea (**2**) with ethyl 2-bromoacetate in glacial acetic acid using sodium acetate as a base. The compound **3** thus formed was condensed with 3-(aryl)-1-phenyl-1*H*-pyrazole-4-carbaldehyde<sup>[42]</sup> (**4a-4g**) in refluxing ethanol using piperidine as a base for 10 to 12 hours. The reaction was monitored by thin-layer chromatography (TLC)

(petroleum ether: ethylacetate [60:40, *v/v*]). Upon completion, the contents of the reaction mass were cooled at room temperature. The solid thus formed was filtered and washed with absolute ethanol to afford thiazolidine-4-one clubbed pyrazole-based molecular hybrids (**THZP1-THZP14**) in 71% to 88% yield (Scheme 1, Table 1).

The structure of all newly synthesized molecular hybrids (**THZP1-THZP14**) was ascertained by using various spectral techniques like infrared (IR), <sup>1</sup>H NMR, and mass. In IR spectrum, N–H stretching and C=O stretching band of the thiazolidinone ring appeared at 3050 to 3127  $\text{cm}^{-1}$  and 1700 to 1720  $\text{cm}^{-1}$ , respectively. The stretching of exocyclic C=C bond present on the thiazolidine-4-one ring resulted into an absorption band in the range 1646 to 1691  $\text{cm}^{-1}$ . Two configurational isomers in terms of *E* and *Z* at the imino form of 2-arylimino-4-thiazolidinone were very well-cited in the literature.<sup>[43]</sup> In case of **3a**, single set of signals was observed, however, for **3b**, two signal sets were observed for –CH<sub>2</sub>, –NH, –OCH<sub>3</sub>, and aryl protons as shown in (Figure 1).

From the above-discussed facts, it was considered that when an electron-withdrawing group such as –NO<sub>2</sub> was present on the phenyl ring, a single set of signals was observed because of the existence of only one configurational isomer, ie, 2*Z*. However, when the electron-withdrawing group was replaced by electron-donating group (–OCH<sub>3</sub>), two sets of signals were observed for two configurational isomers due to restricted rotation about the imine (C=N) linkage, ie, 2*Z* and 2*E*. The presence of two isomeric forms was also observed in case of the target molecular hybrids (**THZP8-THZP14**) synthesized from **3b**.

To understand the configurational isomerism of molecular hybrids (**THZP1-THZP14**) by <sup>1</sup>H NMR, compound 2-(4-methoxyphenylimino)-5-([1-phenyl-3-*p*-tolyl-1*H*-pyrazol-4-yl]methylene)thiazolidin-4-one (**THZP8**)



**Reaction conditions:** (a) KSCN, 6N HCl, 80°C, 8–10 h; (b) BrCH<sub>2</sub>COOEt, glacial acetic acid, CH<sub>3</sub>COONa, reflux 2 h; (c) Piperidine, ethanol, reflux 10–12 h.

**SCHEME 1** Synthesis of thiazolidine-4-one clubbed pyrazole based molecular hybrids (**THZP1-THZP14**)

was taken as a test case. In  $^1\text{H}$  NMR of **THZP8**, peaks at ( $\delta$  3.78–3.77) and ( $\delta$  8.66–8.57) were observed because of  $-\text{OMe}$  and  $\text{Pyr}-\text{H}$  protons, respectively. Aromatic protons of  $2E,5Z$  and  $2Z,5Z$  isomers were also associated with two signal sets for **THZP8** (Figure 2). When the  $^1\text{H}$  NMR of the test compound was recorded in trifluoroacetic acid (TFA), the doubling of resonating signals disappeared, and it clearly shows that the diastereomeric mixture is dynamic not static (Figure 2). The configurational isomerism is also confirmed by 2D- $^1\text{H}$  NMR and HRMS (see Data S1, Figure S20–S23). Resonating signals at  $\delta$  7.46–7.37 ppm in  $^1\text{H}$  NMR was associated with the olefinic proton ( $\text{H}_7$ ). The chemical shift value observed for this proton was higher than expected for  $5E$  isomer and was mainly because of anisotropic effect of  $\text{C}=\text{O}$  present in the vicinity of this proton.<sup>[43]</sup> Further, a proton present in the vicinity of sulfur would resonate at lower  $\delta$  value due to less deshielding effect exerted by sulfur, which was also not observed in present case.<sup>[44]</sup> Therefore, the possibility of isomerization at fifth position was ruled out and only two isomers are possible because of  $\text{C}=\text{N}$  isomerization in condensed

products (**THZP8-THZP14**). Similarly, in case of compounds (**THZP1-THZP14**) the  $\delta$  value observed for  $\text{H}_7$  was also in agreement with the  $Z$  isomer.

Therefore, these compounds exist only in one configurational isomer  $2Z,5Z$ . The existence of two isomeric forms in terms of  $\text{C}=\text{N}$  configurational isomers was supported by the presence of two signal sets when the spectra were recorded in DMSO which is also conferring with the literature.<sup>[43,44]</sup> The predominance of isomer was assessed by integrating the singlets observed for protons related with methoxy ( $-\text{OCH}_3$ ) and pyrazole at  $25^\circ\text{C}$ . The  $2Z,5Z$  isomer was found to be predominant with a percentage of 58.47% to 60.59%. However, the relative percentage observed for  $2E,5Z$  isomer was 39.41% to 41.17%. (Table S1).

## 2.2 | Configurational studies using DFT

The molecular geometry of all the newly synthesized compounds (**THZP1-THZP14**) was optimized with DFT. B3LYP exchange-correlation functional<sup>[45,46]</sup> along with 6-311G basic sets were used through Gaussian09 package. Initially, analysis of  $^1\text{H}$  NMR reveals the possibility of two isomeric forms for compound **3b** and one for **3a**. Moreover, after its condensation with an aldehyde at fifth position, two more isomeric form results due to  $\text{C}=\text{C}$  isomerization at fifth position. However, the  $^1\text{H}$  NMR of the compound **THZP8** reveals the presence of only two isomeric forms which are possible only because of  $\text{C}=\text{N}$  isomerization. The two isomeric forms were then constructed with full energy optimizations performed by using same correlation functional. No imaginary frequencies were observed on their respective potential energy surfaces, which ensure the energy minima for all isomers. Out of these, the isomer with ( $2Z,5Z$ ) configuration is of lowest energy and is more stable. The comparative analysis of the total energy ( $E_{\text{total}}$ ) for ( $2Z,5Z$ ) and ( $2E,5Z$ ) of **THZP1** and **THZP8** was done and the results were tabulated in Table 2. The  $E_{\text{rel}}$  observed for ( $2E,5Z$ ) isomer was 3.75 kcal/mol for **THZP1** and 11.15 kcal/mol than ( $2E,5Z$ ) for **THZP8**, respectively, which suggests configurational barrier between two isomers of **THZP8** because of comparatively high energy gap between them. The

**TABLE 1** Synthesis of thiazolidine-4-one clubbed pyrazole based molecular hybrids (**THZP1-THZP14**)

S. No.	Compound Code	—R	—R <sub>1</sub>	Yield, %
1.	<b>THZP1</b>	—NO <sub>2</sub>	—OCH <sub>3</sub>	85
2.	<b>THZP2</b>	—NO <sub>2</sub>	—F	81
3.	<b>THZP3</b>	—NO <sub>2</sub>	—Cl	83
4.	<b>THZP4</b>	—NO <sub>2</sub>	—Br	75
5.	<b>THZP5</b>	—NO <sub>2</sub>	—CH <sub>3</sub>	82
6.	<b>THZP6</b>	—NO <sub>2</sub>	—H	77
7.	<b>THZP7</b>	—NO <sub>2</sub>	—NO <sub>2</sub>	88
8.	<b>THZP8</b>	—OCH <sub>3</sub>	—CH <sub>3</sub>	80
9.	<b>THZP9</b>	—OCH <sub>3</sub>	—OCH <sub>3</sub>	75
10.	<b>THZP10</b>	—OCH <sub>3</sub>	—Br	71
11.	<b>THZP11</b>	—OCH <sub>3</sub>	—F	78
12.	<b>THZP12</b>	—OCH <sub>3</sub>	—Cl	85
13.	<b>THZP13</b>	—OCH <sub>3</sub>	—H	79
14.	<b>THZP14</b>	—OCH <sub>3</sub>	—NO <sub>2</sub>	83

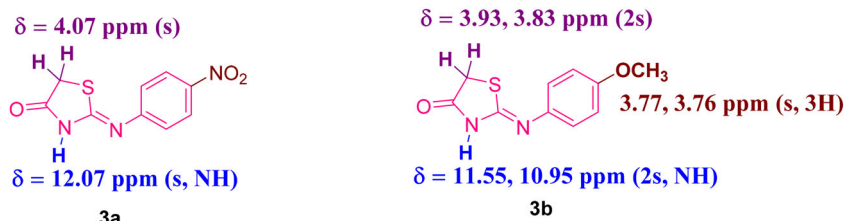


**FIGURE 1** Two signal sets assigned for **3a** and **3b** in  $^1\text{H}$  NMR [Color figure can be viewed at [wileyonlinelibrary.com](http://wileyonlinelibrary.com)]

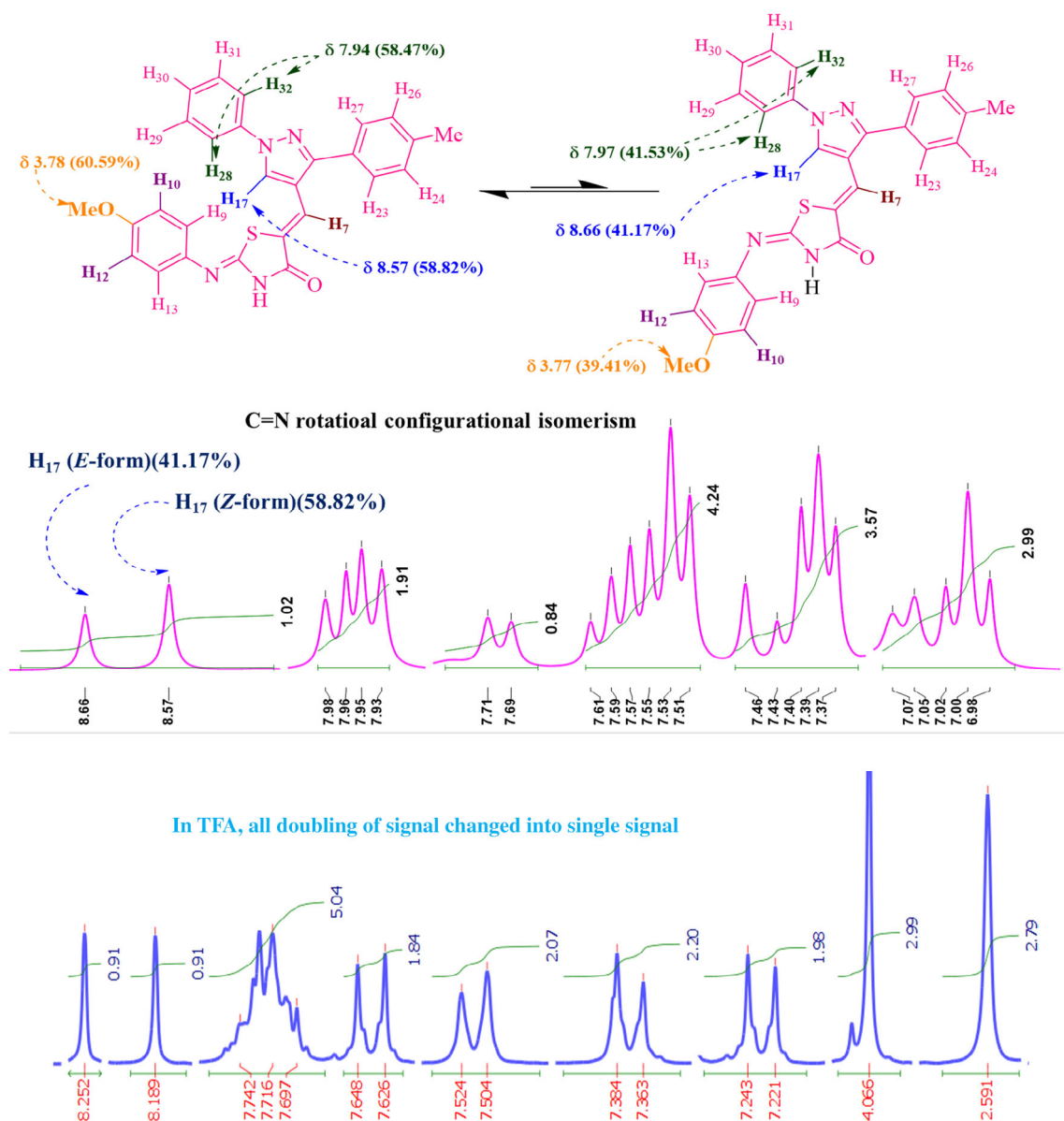


**FIGURE 2** Configurational isomerism in **THZP8** with the characteristic peak in its  $^1\text{H}$  NMR in  $\text{DMSO-}d_6$  and trifluoroacetic acid (TFA) [Color figure can be viewed at [wileyonlinelibrary.com](http://wileyonlinelibrary.com)]

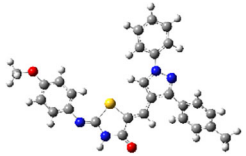
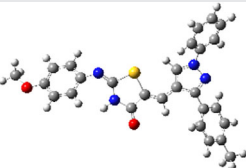
geometry optimization was then performed using 2Z,5Z configuration for all compounds and their optimized geometry with energy and dipole moment are tabulated in Table S2.

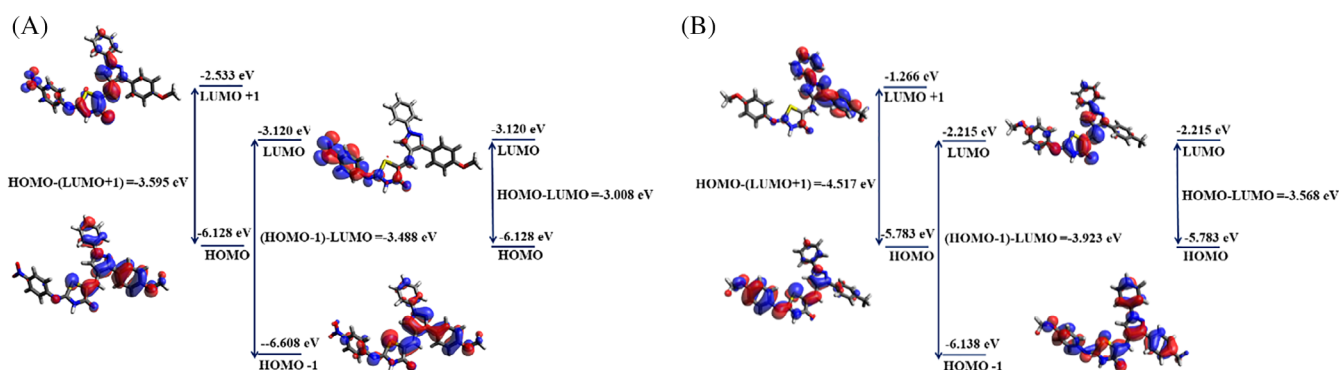
### 2.3 | Electrostatic results

The physicochemical behaviour, energy gap, and energy associated with a compound can be best defined using energy of molecular orbitals. The eigen value associated with these frontier molecular orbitals was then assessed to furnish the chemical reactivity and biological potency of a molecule.<sup>[47]</sup> HOMO and LUMO for **THZP1** and

**THZP8** are shown in Figure 3. DFT-based global reactivity descriptors, ie, chemical hardness ( $\eta$ ), chemical potential ( $\mu$ ), electrophilicity index ( $\omega$ ), and electronegativity ( $\chi$ ) have been quite extensively studied to predict the bioprofile of a molecule.<sup>[48–50]</sup> The chemical hardness of a system is an important parameter for accessing the stability and reactivity of a system and is represented by  $\eta = (E_{\text{LUMO}} - E_{\text{HOMO}})/2$ . This descriptor is used as a measure of resistance to change in the electronic distribution or charge on a molecule.<sup>[51]</sup> Electronegativity, another global reactivity descriptor represented by  $\chi = -(E_{\text{HOMO}} + E_{\text{LUMO}})/2$ , is defined as the electron attracting ability of an atom in a molecule.<sup>[52]</sup>

**TABLE 2** Configurational barrier in terms of relative energies for two isomeric forms of compound **THZP1** and **THZP8**

Isomeric form	Isomers of <b>THZP1</b>	$E_{\text{total}}$ (au)	$E_{\text{rel}}$ Kcal/mol	Isomers of <b>THZP8</b>	$E_{\text{total}}$ (au)	$E_{\text{rel}}$ Kcal/mol
2Z,5Z		-1974.85458	0.0		-1809.68703	0.0
2E,5Z		-1974.84860	3.75		-1809.66925	11.15

**FIGURE 3** HOMO-LUMO for compound (A) **THZP1** and (B) **THZP8** [Color figure can be viewed at [wileyonlinelibrary.com](http://wileyonlinelibrary.com)]

Further, the negative of electronegativity is known as chemical potential<sup>[53]</sup> and is defined as  $\mu = (E_{\text{HOMO}} + E_{\text{LUMO}})/2$ . The global electrophilic nature associated with a molecule can be assessed in a relative range using electrophilicity index ( $\omega$ ). This descriptor was introduced by Parr and is calculated using the electronic chemical potential and chemical hardness and given as  $\omega = \mu^2/2\eta$ .<sup>[54]</sup> All the values of global reactivity descriptors calculated for all the newly synthesized compounds (**THZP1-THZP14**) are summarized in Table 3.

These molecular hybrids (**THZP1-THZP8**) are categorized into two series according to the structural homology: both series I and II consists of seven compounds each. Series I (**THZP1-THZP8**), where aryl group of thiazolidine-4-one is substituted with nitro group, differs from series II (**THZP8-THZP14**) in terms of substituent present on the aryl group of thiazolidine-4-one. Compounds substituted with methoxy group on the aryl group of thiazolidine-4-one are categorized under series II. From Table 3, it has been revealed that the highest value of hardness was associated with **THZP7** (5.03 eV)

and lowest with **THZP1** (4.62 eV) among the compounds of series I with a difference of 0.41 eV between two extreme values. However, this difference became 0.59 eV in series II with the highest hardness value of 4.56 eV corresponds to **THZP14** (4.56 eV) and the lowest with **THZP9** (3.97 eV). From the above discussion and on the basis of principle of maximum hardness, it has been revealed that compounds **THZP7** and **THZP14** are more reactive than **THZP1** and **THZP9**. Highest electron attracting capabilities were observed for **THZP7** and **THZP14** with electronegativity values of 2.51 and 2.28 eV, respectively, in their respective series.

Further, high value of electrophilicity index ( $\omega$ ) associated with both compounds reflects their strong electrophilic abilities. The relative change between extreme values of electrophilicity index ( $\omega$ ) ( $\omega_{\text{max}} - \omega_{\text{min}} / \omega_{\text{max}}$ ) was smaller for series I (0.07) as compared with series II (0.13). This higher value of relative change associated with series II reflects its strong capacity to accept electrons than series I with more sensitivity towards specific substituents (Table 3).

Molecules with a  $\pi$ -conjugated system may result in asymmetric polarisation because of the presence of electron releasing and withdrawing substituents. Materials accompanying high NLO properties can be applied in optoelectronic and nonlinear optics. In order to investigate the NLO properties associated with compounds (THZP1-THZP14), DFT method was employed to calculate the polarizabilities and hyperpolarizabilities associated with compounds (THZP1-THZP14). The various

parameters like dipole moment ( $\mu$ ), polarizability ( $\alpha$ ), and its first-order component ( $\beta$ ) calculated for all the compounds (THZP1-THZP14) are listed in Table 4. The values associated with  $\alpha$  and  $\beta$  were reported in e.s.u. Conversion factor  $0.1482 \times 10^{-24}$  e.s.u for  $\Delta\alpha$  and  $8.6393 \times 10^{-33}$  e.s.u for  $\beta_{\text{tot}}$  were used for conversion of values observed in atomic units (au). The calculated values were then compared with the standard prototype, ie, urea.

**TABLE 3** Electrostatic results for compounds THZP1-THZP14

Compounds	HOMO	LUMO	HOMO-1	LUMO +1	Chemical Potential, $\mu$	Global Hardness $\eta = (-\mu)$	Global Electrophilicity Index ( $\omega$ ) = $\mu^2/2\eta$	Softness (s) $s = 1/\eta$
THZP1	-6.13	-3.10	-6.61	-2.53	-4.62	4.62	2.31	0.22
THZP2	-6.48	-3.19	-7.06	-2.66	-4.84	4.84	2.42	0.21
THZP3	-6.52	-3.21	-7.07	-2.69	-4.86	4.86	2.43	0.21
THZP4	-6.48	-3.20	-6.98	-2.67	-4.84	4.84	2.42	0.21
THZP5	-6.30	-3.12	-6.84	-2.55	-4.71	4.71	2.35	0.21
THZP6	-6.38	-3.14	-6.97	-2.57	-4.76	4.76	2.38	0.21
THZP7	-6.73	-3.33	-7.28	-3.25	-5.03	5.03	2.52	0.20
THZP8	-5.78	-2.22	-6.14	-1.27	-4.00	4.00	2.00	0.25
THZP9	-5.74	-2.20	-5.99	-1.22	-3.97	3.97	1.98	0.25
THZP10	-5.89	-2.34	-6.29	-1.50	-4.12	4.11	2.06	0.24
THZP11	-5.89	-2.34	-6.29	-1.47	-4.12	4.12	2.06	0.24
THZP12	-5.91	-2.36	-6.33	-1.53	-4.14	4.14	2.07	0.24
THZP13	-5.82	-2.25	-6.25	-1.31	-4.03	4.03	2.02	0.25
THZP14	-6.02	-3.11	-2.49	-6.53	-4.56	4.56	2.28	0.22

**TABLE 4** NLO properties associated with compounds (THZP1-THZP14)

Compound	Dipole Moment, $\mu$	$\beta_{\text{tot}}$ (au)	$\beta_{\text{tot}} \times 10^{-30}$ (e.s.u)	$\langle\alpha\rangle$ (au)	$\langle\Delta\alpha\rangle$ (au)	$\langle\Delta\alpha\rangle \times 10^{-24}$ (e.s.u)
THZP1	6.36	986.92	8.52	-223.31	56.26	8.34
THZP2	2.93	389.32	3.36	-229.29	99.47	14.74
THZP3	2.74	368.66	3.18	-239.12	104.72	15.52
THZP4	3.03	979.41	8.46	-242.96	98.23	14.56
THZP5	5.32	706.86	6.10	-220.41	57.98	8.59
THZP6	4.71	586.26	5.06	-215.05	63.99	9.48
THZP7	3.91	256.88	2.21	-256.02	146.00	21.64
THZP8	3.76	312.19	2.69	-189.29	50.06	7.42
THZP9	3.44	240.35	2.07	-190.69	65.27	9.67
THZP10	6.74	286.42	2.47	-206.70	36.28	5.38
THZP11	6.81	617.96	5.33	-197.68	34.29	5.08
THZP12	7.37	730.13	6.30	-206.02	35.47	5.26
THZP13	4.31	400.55	3.46	-183.38	49.79	7.38
THZP14	11.10	1207.05	10.42	-221.71	57.03	8.45

All the compounds showed many fold NLO properties when compared with urea ( $0.15 \times 10^{-30}$ ) (Table 4). It has been revealed from Table 4 that compounds substituted with electron-releasing group at one end and electron-withdrawing at the other are associated with high second-order nonlinear optical properties. Among all, compound **THZP14** showed highest  $\beta_{\text{tot}}$  (e.s.u) value of  $10.42 \times 10^{-30}$ , which is nearly 70 times more than urea, followed by **THZP1** with  $\beta_{\text{tot}}$  (e.s.u) value of  $8.52 \times 10^{-30}$ . The pattern of substitution plays an important role here. Compounds substituted with nitro group on pyrazole ring and methoxy group on phenyl ring attached with thiazolidine-4-one (**THZP14**) showed highest  $\beta_{\text{tot}}$  (e.s.u) value. However, a decrease in the value of  $\beta_{\text{tot}}$  (e.s.u) from  $10.42 \times 10^{-30}$  to  $8.52 \times 10^{-30}$  was observed when the pattern of substitution was reversed. Above findings suggests that the asymmetric polarization resulted to a maximum extent when electron density flows in a direction from thiazolidine-4-one to pyrazole ring. Moreover, compounds with substitution of similar nature are also associated with low value of  $\beta_{\text{tot}}$  (e.s.u), ie, **THZP7** and **THZP9**.

## 2.4 | Biological studies

### 2.4.1 | Enzyme inhibition studies

The aim behind design and synthesis of thiazolidine-4-one clubbed pyrazole would be incomplete without exploring their biological potential. Towards this, screening was done for evaluating the inhibitory potential of molecular hybrids against  $\alpha$ -amylase and  $\alpha$ -glucosidase enzyme. The inhibition showed by all the hybrids was also compared with standard drug acarbose. The  $\text{IC}_{50}$  values were determined for all the newly synthesized molecular hybrids against  $\alpha$ -amylase and  $\alpha$ -glucosidase. As shown in Table 5, the  $\text{IC}_{50}$  varied from  $9.90\mu\text{M}$  to  $65.02\mu\text{M}$  for  $\alpha$ -amylase and from  $4.48\mu\text{M}$  to  $92.32\mu\text{M}$  for  $\alpha$ -glucosidase, respectively. Significant inhibition was observed for all the compounds when compared with standard. In case of  $\alpha$ -amylase, all compounds except **5e** ( $\text{IC}_{50} = 65.02\mu\text{M}$ ) showed improved  $\text{IC}_{50}$  value when compared with standard drug acarbose. However, in case of  $\alpha$ -glucosidase, compounds **THZP14**, **THZP13**, **THZP8**, and **THZP3** showed comparable inhibition with  $\text{IC}_{50}$  value of  $4.48\mu\text{M}$ ,  $14.86\mu\text{M}$ ,  $8.60\mu\text{M}$ , and  $13.26\mu\text{M}$ , respectively. In case of  $\alpha$ -amylase, the most potent compound was **THZP9** with  $\text{IC}_{50} = 9.90\mu\text{M}$ . However, in case of  $\alpha$ -glucosidase, the most potent was **THZP14** with  $\text{IC}_{50} = 4.48\mu\text{M}$ . The inhibition profile of the all the compounds and their comparison with standard drug was shown in Figure 4.

**TABLE 5** Inhibition profile of compounds (**THZP1-THZP14**) against  $\alpha$ -amylase and  $\alpha$ -glucosidase

Compound	$\alpha$ -Amylase		$\alpha$ -Glucosidase	
	$\text{IC}_{50}$ ( $\mu\text{M}$ )	SE	$\text{IC}_{50}$ ( $\mu\text{M}$ )	SE
<b>THZP1</b>	14.49	$\pm 2.47$	17.31	$\pm 1.50$
<b>THZP2</b>	43.30	$\pm 1.25$	40.43	$\pm 1.40$
<b>THZP3</b>	51.04	$\pm 1.63$	13.26	$\pm 2.32$
<b>THZP4</b>	25.31	$\pm 1.26$	16.73	$\pm 1.75$
<b>THZP5</b>	65.02	$\pm 1.39$	89.15	$\pm 1.30$
<b>THZP6</b>	13.79	$\pm 2.16$	92.32	$\pm 1.37$
<b>THZP7</b>	14.49	$\pm 1.41$	32.20	$\pm 1.15$
<b>THZP8</b>	28.01	$\pm 1.74$	8.60	$\pm 1.33$
<b>THZP9</b>	9.90	$\pm 1.53$	54.46	$\pm 1.23$
<b>THZP10</b>	38.10	$\pm 1.10$	28.08	$\pm 1.25$
<b>THZP11</b>	13.80	$\pm 1.32$	23.34	$\pm 1.66$
<b>THZP12</b>	10.24	$\pm 3.82$	56.70	$\pm 1.49$
<b>THZP13</b>	11.45	$\pm 1.44$	14.86	$\pm 1.63$
<b>THZP14</b>	16.15	$\pm 1.37$	4.48	$\pm 1.19$
<b>Acarbose</b>	47.86	$\pm 1.36$	10.53	$\pm 1.38$

### 2.4.2 | Molecular docking studies

Recently, the computer-assisted drug design (CADD) has been accepted as a successful methodology of drug design and discovery to understand the structural design of a drug candidate. It is quite fast, cost-effective, and result-oriented fruitful in silico technique.<sup>[55,56]</sup> The active site of a target protein can be assessed using molecular docking to explore the probable binding modes of a drug. The molecular docking studies were performed with AutoDock Vina software to predict the probable mode of binding for most potent compounds **THZP9** and **THZP14**. Docking simulation of **THZP9** and **THZP14** was performed with the active site of *Aspergillus oryzae* from  $\alpha$ -amylase (PDB ID: 7TAA) and  $\alpha$ -glucosidase from *Saccharomyces cerevisiae* to establish the binding conformation and interactions responsible for their activity. The most active compounds **THZP9** and **THZP14** were sketched using ChemAxon software and these were changed into 3D structures using the MMFF94 force field.

### 2.4.3 | Docking analysis of $\alpha$ -amylase

Binding pose with the highest binding affinity for docked conformation of **THZP9** is shown in Figure 5. It has been revealed from Figure 5 that various interactions in terms

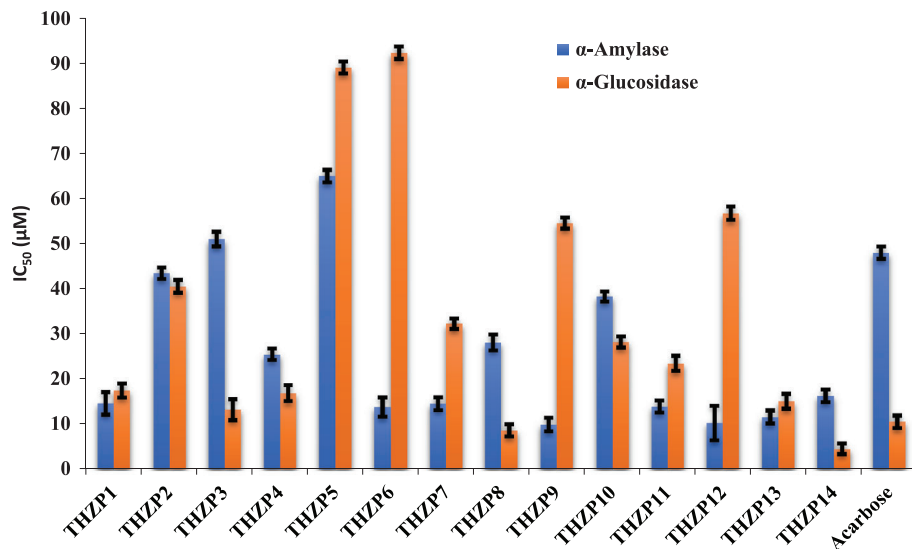


**FIGURE 4** Graphical representation of IC<sub>50</sub> (µM) of compounds (THZP1-THZP14) against α-amylase and α-glucosidase [Color figure can be viewed at wileyonlinelibrary.com]

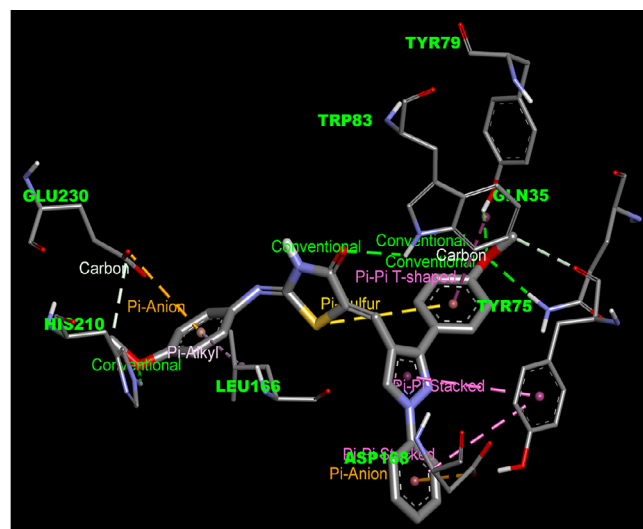
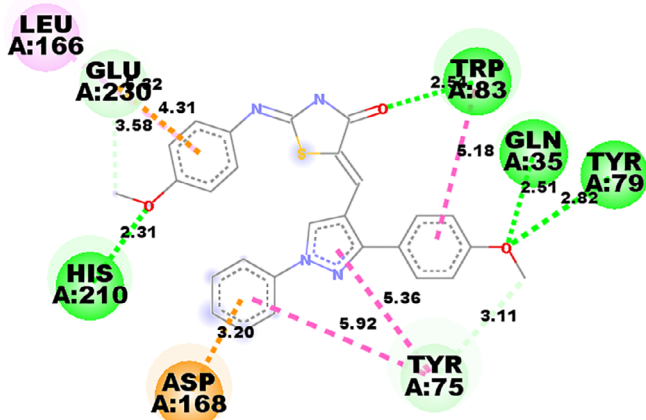


**FIGURE 5** 2D and 3D dock pose of α-amylase with THZP9 [Color figure can be viewed at wileyonlinelibrary.com]

of hydrogen bonding, hydrophobic, electrostatic, and  $\pi$ -sulfur interactions are mainly responsible for anchoring of the compound THZP9 in active site of α-amylase. The oxygen atom of methoxy group and carbonyl group form the conventional hydrogen bonding with the Gln35, Tyr79, Trp83, and His210 amino acid. The oxygen atom act as acceptor and these amino acids act as donor. The carbon-hydrogen bond was found between the carbon of methoxy group and Glu230 and Tyr75. The electrostatic interaction, ie,  $\pi$ -anion was created between the phenyl ring and Asp168 & Glu230 amino acid. The hydrophobic interactions such as  $\pi$ - $\pi$  stacked,  $\pi$ - $\pi$  T-shaped, and  $\pi$ -alkyl were also found (Table S3). In case of α-amylase, Glu230 and Asp206 are the residues responsible for the catalytic activity in hydrolytic reactions<sup>[57]</sup> and the binding of THZP9 to these residues is probably the cause of

inhibition in case of α-amylase. Further, the co-crystallized ligand along with THZP9 in the active site of α-amylase is shown in Figure S1.

#### 2.4.4 | Docking analysis of α-glucosidase

The docking study was performed after the preparation of a homology model for α-glucosidase because of unavailability of the crystal structure for α-glucosidase of *S. cerevisiae* (strain ATCC 204508 / S288c). The α-glucosidase from *S. cerevisiae* [EC: 3.2.1.20] (CAS Number 9001-42-7) was purchased from Sigma Aldrich. The gene information shows that it contains MAL12 (853209) and MAL32 (852602) of baker yeast. The primary sequence of α-glucosidase for *S. cerevisiae* was taken from UniProtKB

(Access code P53341 for MAL12, UniRef100\_P53341, and P38158 for MAL32, UniRef100\_P38158) and BLAST was used to search the template against the PDB. The PDB 3AXH showed 72% identity and 85% similarity with the target enzyme  $\alpha$ -glucosidase and was used as a template for homology modelling. Then, a homology model was prepared using SWISS-MODEL and checked using PROCHECK.<sup>[58]</sup> The result retrieved from PROCHECK in terms of Ramachandran plot revealed that in final 3D structure 89.0% of residues are present in most favoured regions (Figure S2). The stereochemical parameter of the main chain and side chain is given in Table S4. All the stereochemical parameters of the main chain were found inside the main region. The graphical representation of stereochemical parameter of the main chain and side chain is given in Figure S3-S4. The prepared PDB was aligned with PDB:3AXH using Pymol (Figure S5). The active site of  $\alpha$ -glucosidase<sup>[59]</sup> was docked with THZP14 using the Auto Dock Vina.<sup>[60]</sup> Then, docked pose was analyzed using discovery studio R2 client.<sup>[61]</sup>

Six hydrogen bonds, three conventional hydrogen bonds, two carbon-hydrogen bonds, and one  $\pi$ -donor hydrogen bond were identified for the most active compound THZP14 (Figure 6). The conventional hydrogen bonding was found between N—H and active site of  $\alpha$ -glucosidase (Glu276 & Asp 349 amino acids), whereas His-245 amino acid was involved in conventional hydrogen bond with oxygen of nitro group. The C—H bonding was found between the carbon of methoxy group and Asp68 & Gln181 amino acid. The N-phenyl ring of

pyrazole moiety formed the  $\pi$ -donor hydrogen bond with Arg 312. The aromatic ring of imine moiety was involved in  $\pi$ -anionic interaction with another active pocket of  $\alpha$ -glucosidase Asp 214 and Arg439 amino acids (Table S5). Docking studies showed that compound THZP14 was entangled in the active pocket of enzyme with six hydrogen bonds, seven hydrophobic, two electrostatic, and two other interactions. Therefore, the enzymatic action of  $\alpha$ -glucosidase was inhibited through these interactions in a cooperative fashion.

### 3 | EXPERIMENTAL

#### 3.1 | Material and methods

Spectral analysis in terms of IR, <sup>1</sup>H NMR, and mass was done to elucidate the structure of all the newly synthesized compounds. The progress of the reaction was monitored using precoated silica gel aluminium plates (60 F<sub>254</sub>) purchased from MERCK. Open glass capillary tubes were used to determine uncorrected melting points. In IR absorption spectra, the values are expressed as  $\nu_{\max}$  cm<sup>-1</sup> and were obtained using Perkin Elmer FTIR spectrophotometer. <sup>1</sup>H NMR spectral analysis was performed in DMSO-*d*<sub>6</sub> using tetramethylsilane as an internal standard. All the spectra were recorded at 400 and 500 MHz on Bruker (Avance-II). The  $\delta$  and *J* values are expressed in ppm and Hz, respectively. The <sup>13</sup>C NMR spectra were not witnessed because of poor solubility of compounds in

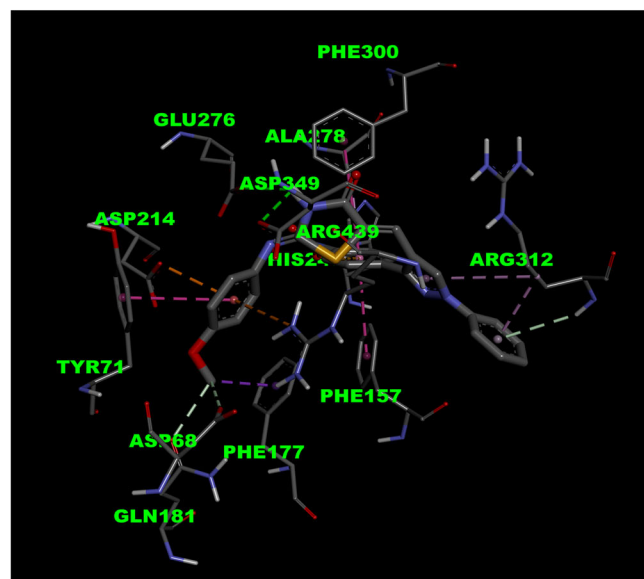
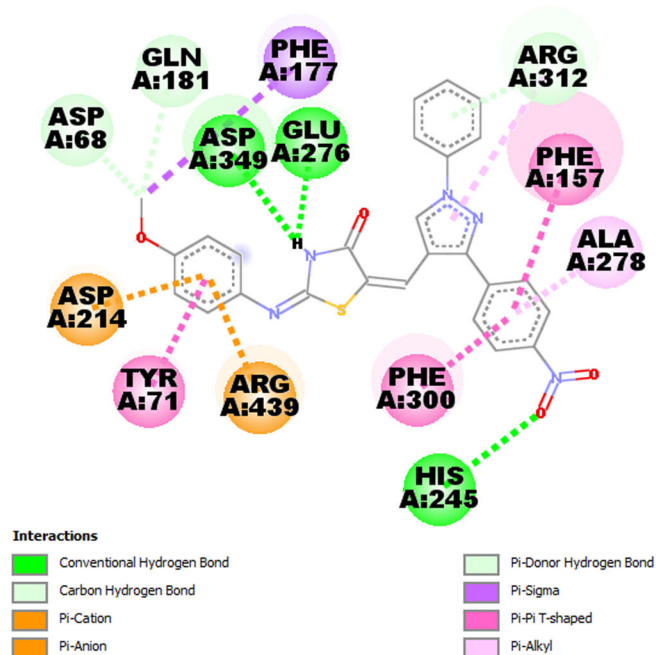


FIGURE 6 2D and 3D-Representation of  $\alpha$ -glucosidase with THZP14 [Color figure can be viewed at wileyonlinelibrary.com]

DMSO- $d_6$  (see Data S1, Figure S24-S37). The chemicals used in the synthesis were procured from local supplier and are of Sigma-Aldrich and MERCK. Waters Micro-mass Q-ToF was used to record mass spectrum. Arylthiourea and substituted pyrazolyl carbaldehydes were prepared using reported procedure.<sup>[22,42]</sup>

### 3.2 | A general method for the synthesis of 2-substituted thiazolidin-4-one (3)<sup>[22]</sup>

A mixture of arylthiourea (1.00 mmol), ethyl bromoacetate (1.00 mmol), and sodium acetate (2.0 mmol) in glacial acetic acid (10 mL) was heated under reflux in a 50-mL round bottom flask. After completion of the reaction (monitored by TLC), the content of the reaction was poured in a beaker containing ice and the solid thus obtained was filtered and recrystallized from ethanol.

### 3.3 | General method for the synthesis of 5-((3-(aryl)-1-phenyl-1H-pyrazol-4-yl)methylene)-2-(p-arylimino)thiazolidin-4-one (THZP1-THZP14)<sup>[22]</sup>

A condensation reaction of 2-arylimino-thiazolidine-4-ones (3) (0.50 mmol) was attempted with substituted pyrazole-4-carbaldehydes (**4a-4g**) (0.50 mmol) in absolute ethanol using piperidine (0.50 mmol) as base. The content of the reaction was stirred for 8 hours at 60°C in a 100-mL round bottom flask. After completion of the reaction, the mixture was allowed to cool at room temperature and the precipitates thus formed were filtered and washed with absolute ethanol to afford the final products (THZP1-THZP14) in good to excellent yield.

## 3.4 | Spectral data

### 3.4.1 | 2-(4-Nitrophenylimino)thiazolidin-4-one (3a)

Yield: 85%; mp 167-170°C; <sup>1</sup>H NMR ( $\delta_{\text{ppm}}$ , 500 MHz, DMSO- $d_6$ ):  $\delta$  11.64 (s, 1H, —NH), 8.41-8.43 (d,  $J$  = 10 Hz, 2H), 7.64-7.66 (d,  $J$  = 10 Hz, 2H), 4.27 (s, 2H, —CH<sub>2</sub>).

### 3.4.2 | 2-(4-Methoxyphenylimino)thiazolidin-4-one (3b)

Yield: 85%; mp 157-160°C; <sup>1</sup>H NMR ( $\delta_{\text{ppm}}$ , 400 MHz, DMSO- $d_6$ ):  $\delta$  11.54, 10.94 (2s, NH), 7.63-7.61 (d,

$J$  = 8.8 Hz, 1H), 6.99-7.01(d,  $J$  = 8.8 Hz, 1H), 6.90-6.87 (m, 2H), 3.93, 3.86 (2s, 2H, —CH<sub>2</sub>), 3.77, 3.76 (2s, 3H, —OCH<sub>3</sub>).

### 3.4.3 | 5-((3-[4-Methoxyphenyl]-1-phenyl-1H-pyrazol-4-yl)methylene)-2-(4-nitrophenylimino)thiazolidin-4-one (THZP1)

Yield: 85%; mp >300°C; IR ( $\nu_{\text{max}}$  cm<sup>-1</sup>, KBr): 3117 (N—H lactam), 1697 (C=O lactam), 1659 (C=C), 1582 (C=N), Ar—NO<sub>2</sub> 1335 (Sym), 1504 (Asym); <sup>1</sup>H NMR ( $\delta_{\text{ppm}}$ , 400 MHz, DMSO- $d_6$ , ppm):  $\delta$  8.59 (1H, s, H<sub>17</sub>), 8.27 (2H, d,  $J$  = 9.2, H<sub>10</sub>/H<sub>12</sub>), 7.94 (2H, d,  $J$  = 8.0, H<sub>28</sub>/H<sub>32</sub>), 7.60-7.50 (7H, m, H<sub>23</sub>/H<sub>27</sub>, H<sub>9</sub>/H<sub>13</sub>, H<sub>29</sub>/H<sub>31</sub>, H<sub>7</sub>), 7.39 (1H, t,  $J$  = 7.4, H<sub>30</sub>), 7.15-7.11 (2H, m, H<sub>24</sub>/H<sub>26</sub>), 3.85 (3H, s, -OCH<sub>3</sub>); Anal. Calc for C<sub>26</sub>H<sub>19</sub>N<sub>5</sub>O<sub>4</sub>S: C, 62.77; H, 3.85; N, 14.08; Found: C, 62.71; H, 3.82; N, 14.06.

### 3.4.4 | 5-((3-[4-Fluorophenyl]-1-phenyl-1H-pyrazol-4-yl)methylene)-2-(4-nitrophenylimino)thiazolidin-4-one (THZP2)

Yield: 81%; mp >300°C; IR ( $\nu_{\text{max}}$  cm<sup>-1</sup>, KBr): 3127 (N—H lactam), 1704 (C=O lactam), 1666 (C=C), 1582 (C=N), Ar—NO<sub>2</sub> 1335 (Sym), 1504 (Asym); <sup>1</sup>H NMR ( $\delta_{\text{ppm}}$ , 400 MHz, DMSO- $d_6$ ):  $\delta$  8.47 (1H, s, H<sub>17</sub>), 8.20 (2H, d,  $J$  = 10.8, H<sub>10</sub>/H<sub>12</sub>), 7.89 (2H, d,  $J$  = 8.0, H<sub>28</sub>/H<sub>32</sub>), 7.68-7.665 (2H, m, H<sub>23</sub>/H<sub>27</sub>), 7.52-7.45 (5H, m, H<sub>9</sub>/H<sub>13</sub>, H<sub>29</sub>/H<sub>31</sub>, H<sub>7</sub>), 7.37-7.30 (3H, m, H<sub>30</sub>, H<sub>24</sub>/H<sub>26</sub>); Anal. Calc for C<sub>25</sub>H<sub>16</sub>FN<sub>5</sub>O<sub>3</sub>S: C, 61.85; H, 3.32; N, 14.43; Found: C, 61.81; H, 3.29; N, 14.41.

### 3.4.5 | 5-((3-[4-Chlorophenyl]-1-phenyl-1H-pyrazol-4-yl)methylene)-2-(4-nitrophenylimino)thiazolidin-4-one (THZP3)

Yield: 83%; mp >300°C; IR ( $\nu_{\text{max}}$  cm<sup>-1</sup>, KBr): 31.24 (N—H lactam), 1744 (C=O lactam), 1697 (C=C), 1582 (C=N), Ar—NO<sub>2</sub> 1335 (Sym), 1504 (Asym); <sup>1</sup>H NMR ( $\delta_{\text{ppm}}$ , 400 MHz, DMSO- $d_6$ )  $\delta$  12.31 (1H, s, —NH), 8.35 (1H, s, H<sub>17</sub>), 8.09 (2H, d,  $J$  = 8.8, H<sub>10</sub>/H<sub>12</sub>), 7.73 (2H, d,  $J$  = 8.0, H<sub>28</sub>/H<sub>32</sub>), 7.47 (2H, d,  $J$  = 8.4, H<sub>9</sub>/H<sub>13</sub>), 7.43-7.29 (5H, m, H<sub>23</sub>/H<sub>27</sub>, H<sub>29</sub>/H<sub>31</sub>, H<sub>30</sub>), 7.21-7.17 (2H, m, H<sub>24</sub>/H<sub>26</sub>), 7.06 (1H, s, H<sub>7</sub>); Anal. Calc for C<sub>25</sub>H<sub>16</sub>ClN<sub>5</sub>O<sub>3</sub>S: C, 59.82; H, 3.21; N, 13.95; Found: C, 59.78; H, 3.19; N, 13.91.

### 3.4.6 | 5-((3-[4-Bromophenyl]-1-phenyl-1H-pyrazol-4-yl)methylene)-2-(4-nitrophenylimino)thiazolidin-4-one (THZP4)

Yield: 75%; mp >300°C; IR ( $\nu_{max}$  cm<sup>-1</sup>, KBr): 3124 (N—H lactam), 1744 (C=O lactam), 1697 (C=C), 1582 (C=N), Ar—NO<sub>2</sub> 1335 (Sym), 1504 (Asym); <sup>1</sup>H NMR ( $\delta_{ppm}$ , 400 MHz, DMSO-*d*<sub>6</sub>):  $\delta$  12.42 (1H, s, —NH), 8.56 (1H, s, H<sub>17</sub>), 8.26 (2H, d, *J* = 9.2, H<sub>10</sub>/H<sub>12</sub>), 7.91 (2H, d, *J* = 7.6, H<sub>28</sub>/H<sub>32</sub>), 7.73 (2H, d, *J* = 8.4, H<sub>9</sub>/H<sub>13</sub>), 7.58 (2H, d, *J* = 8.4, H<sub>23</sub>/H<sub>27</sub>), 7.53-7.49 (4H, m, H<sub>29</sub>/H<sub>31</sub>, H<sub>24</sub>/H<sub>26</sub>), 7.39-7.35 (2H, m, H<sub>30</sub>, H<sub>7</sub>); Anal. Calc for C<sub>25</sub>H<sub>16</sub>BrN<sub>5</sub>O<sub>3</sub>S: C, 54.95; H, 2.95; N, 12.82; Found: C, 54.94; H, 2.91; N, 12.76.

### 3.4.7 | 2-(4-Nitrophenylimino)-5-([1-phenyl-3-*p*-tolyl-1H-pyrazol-4-yl)methylene)thiazolidin-4-one (THZP5)

Yield: 82%; mp >300°C; IR ( $\nu_{max}$  cm<sup>-1</sup>, KBr): 3124 (N—H lactam), 1697 (C=O lactam), 1659 (C=C), 1582 (C=N), Ar—NO<sub>2</sub> 1335 (Sym), 1504 (Asym); <sup>1</sup>H NMR ( $\delta_{ppm}$ , 400 MHz, DMSO-*d*<sub>6</sub>):  $\delta$  12.44 (1H, s, —NH), 8.51 (1H, s, H<sub>17</sub>), 8.27 (2H, d, *J* = 8.8, H<sub>10</sub>/H<sub>12</sub>), 7.91 (2H, d, *J* = 8.0, H<sub>28</sub>/H<sub>32</sub>), 7.55-7.49 (6H, m, H<sub>9</sub>/H<sub>13</sub>, H<sub>23</sub>/H<sub>27</sub>, H<sub>7</sub>, H<sub>30</sub>), 7.39-7.35 (4H, m, H<sub>29</sub>/H<sub>31</sub>, H<sub>24</sub>/H<sub>26</sub>), 2.42 (3H, s, CH<sub>3</sub>); Anal. Calc for C<sub>26</sub>H<sub>19</sub>N<sub>5</sub>O<sub>3</sub>S: C, 64.85; H, 3.98; N, 14.54; Found: C, 64.83; H, 3.91; N, 14.51.

### 3.4.8 | 5-([1,3-Diphenyl-1H-pyrazol-4-yl)methylene)-2-(4-nitrophenylimino)thiazolidin-4-one (THZP6)

Yield: 77%; mp >300°C; IR ( $\nu_{max}$  cm<sup>-1</sup>, KBr): 3124 (N—H lactam), 1744 (C=O lactam), 1666 (C=C), 1582 (C=N), Ar—NO<sub>2</sub> 1335 (Sym), 1504 (Asym); <sup>1</sup>H NMR ( $\delta_{ppm}$ , 400 MHz, DMSO-*d*<sub>6</sub>):  $\delta$  8.37 (s, 1H, H<sub>17</sub>), 8.23 (d, *J* = 9.2 Hz, 2H, H<sub>10</sub>/H<sub>12</sub>), 7.84 (d, *J* = 8.4 Hz, 2H, H<sub>28</sub>/H<sub>32</sub>), 7.61-7.44 (m, 8H, H<sub>23</sub>/H<sub>27</sub>, H<sub>9</sub>/H<sub>13</sub>, H<sub>29</sub>/H<sub>31</sub>, H<sub>7</sub>, H<sub>30</sub>), 7.35-7.19 (m, 3H, H<sub>24</sub>/H<sub>26</sub>, H<sub>25</sub>); Anal. Calc. For C<sub>25</sub>H<sub>17</sub>N<sub>5</sub>O<sub>3</sub>S: C, 64.23; H, 3.67; N, 14.98; Found: C, 64.22; H, 3.65; N, 14.92.

### 3.4.9 | 5-((3-[4-Nitrophenyl]-1-phenyl-1H-pyrazol-4-yl)methylene)-2-(4-nitrophenylimino)thiazolidin-4-one (THZP7)

Yield: 88%; mp >300°C; IR ( $\nu_{max}$  cm<sup>-1</sup>, KBr): 3117 (N—H lactam), 1744 (C=O lactam), 1705 (C=C), 1682 (C=N),

Ar—NO<sub>2</sub> 1342 (Sym), 1512 (Asym); <sup>1</sup>H NMR ( $\delta_{ppm}$ , 400 MHz, DMSO-*d*<sub>6</sub>):  $\delta$  8.54 (s, 1H, H<sub>17</sub>), 8.39 (d, *J* = 8.8 Hz, 2H, H<sub>24</sub>/H<sub>26</sub>), 8.24 (d, *J* = 8.9 Hz, 2H, H<sub>10</sub>/H<sub>12</sub>), 7.96-7.91 (m, 4H, H<sub>23</sub>/H<sub>27</sub>, H<sub>28</sub>/H<sub>32</sub>), 7.57-7.52 (m, 5H, H<sub>9</sub>/H<sub>13</sub>, H<sub>29</sub>/H<sub>31</sub>, H<sub>7</sub>), 7.41-7.38 (m, 1H, H<sub>30</sub>); Anal. Calc. For C<sub>25</sub>H<sub>16</sub>N<sub>6</sub>O<sub>5</sub>S: C, 58.59; H, 3.15; N, 16.40; Found: C, 58.55; H, 3.13; N, 16.38.

### 3.4.10 | 2-(4-Methoxyphenylimino)-5-([1-phenyl-3-*p*-tolyl-1H-pyrazol-4-yl)methylene)thiazolidin-4-one (THZP8)

Yield: 80%; mp 295-296°C; IR ( $\nu_{max}$  cm<sup>-1</sup>, KBr): 3114 (N—H lactam), 1736 (C=O lactam), 1643 (C=C), 1605 (C=N); <sup>1</sup>H NMR ( $\delta_{ppm}$ , 400 MHz, DMSO-*d*<sub>6</sub>):  $\delta$  8.66, 8.57 (2s, 41.17% (*E*), 58.82% (*Z*), 1H, H<sub>17</sub>), 7.97 (d, 2H, *J* = 7.6 Hz, 41.53% (*E*), H<sub>28</sub>/H<sub>32</sub>), 7.94 (d, 2H, *J* = 7.6 Hz, 58.47% (*Z*), H<sub>28</sub>/H<sub>32</sub>), 7.71-7.51 (m, 6H, H<sub>9</sub>/H<sub>13</sub>, H<sub>23</sub>/H<sub>27</sub>, H<sub>29</sub>/H<sub>31</sub>), 7.46-7.37 (m, 6H, H<sub>7</sub>, H<sub>30</sub>, H<sub>9</sub>/H<sub>13</sub>, H<sub>10</sub>/H<sub>12</sub>), 7.07-6.98 (m, 4H, H<sub>24</sub>/H<sub>26</sub>, H<sub>10</sub>/H<sub>12</sub>), 3.78, 3.77 (2s, 3H, 60.59% (*Z*), 39.41% (*E*), OCH<sub>3</sub>), 2.41 (s, 3H, CH<sub>3</sub>); Anal. Calc. For C<sub>27</sub>H<sub>22</sub>N<sub>4</sub>O<sub>2</sub>S: C, 69.51; H, 4.75; N, 12.01; Found: C, 69.45; H, 4.68; N, 11.97.

### 3.4.11 | 5-((3-[4-Methoxyphenyl]-1-phenyl-1H-pyrazol-4-yl)methylene)-2-(4-methoxyphenylimino)thiazolidin-4-one (THZP9)

Yield: 75%; mp 299-300°C; IR ( $\nu_{max}$  cm<sup>-1</sup>, KBr): 3070 (N—H lactam), 1720 (C=O lactam), 1651 (C=C), 1612 (C=N); <sup>1</sup>H NMR ( $\delta_{ppm}$ , 500 MHz, DMSO-*d*<sub>6</sub>):  $\delta$  8.64, 8.56 (2s, 1H, 40.95% (*E*), 59.05% (*Z*), H<sub>17</sub>), 7.97 (d, *J* = 8.0 Hz, 2H, 41.51% (*E*), H<sub>28</sub>/H<sub>32</sub>), 7.93 (d, *J* = 8.0 Hz, 2H, 58.48% (*Z*), H<sub>28</sub>/H<sub>32</sub>), 7.69-7.51 (m, 6H, H<sub>9</sub>/H<sub>13</sub>, H<sub>23</sub>/H<sub>27</sub>, H<sub>29</sub>/H<sub>31</sub>), 7.45-7.36 (m, 2H, H<sub>7</sub>, H<sub>30</sub>), 7.15-7.12 (m, 2H, H<sub>24</sub>/H<sub>26</sub>), 7.06-7.04 (d, *J* = 8.5 Hz, 2H, 39.69% (*E*), H<sub>10</sub>/H<sub>12</sub>), 7.00-6.97 (m, 4H, H<sub>9</sub>/H<sub>13</sub>, 60.31% (*Z*), H<sub>10</sub>/H<sub>12</sub>), 3.85 (s, 3H, OCH<sub>3</sub>), 3.78, 3.71 (2s, 3H, 61.76% (*Z*), 38.24% (*E*), OCH<sub>3</sub>); Anal. Calc for C<sub>27</sub>H<sub>22</sub>N<sub>4</sub>O<sub>3</sub>S: C, 67.20; H, 4.60; N, 11.61; Found: C, 67.16; H, 4.58; N, 11.60.

### 3.4.12 | 5-((3-[4-Bromophenyl]-1-phenyl-1H-pyrazol-4-yl)methylene)-2-(4-methoxyphenylimino)thiazolidin-4-one (THZP10)

Yield: 71%; mp >300°C; IR ( $\nu_{max}$  cm<sup>-1</sup>, KBr): 3047 (N—H lactam), 1713 (C=O lactam), 1654 (C=C), 1605 (C=N); <sup>1</sup>H NMR ( $\delta_{ppm}$ , 500 MHz, DMSO-*d*<sub>6</sub>):  $\delta$  8.69, 8.61 (2s, 1H, 41.58% (*E*), 58.42% (*Z*), H<sub>17</sub>), 7.98 (d, *J* = 8.5 Hz, 2H,

41.55% (*E*), H<sub>28</sub>/H<sub>32</sub>), 7.94 (d, *J* = 8.0 Hz, 2H, 58.44% (*Z*), H<sub>28</sub>/H<sub>32</sub>), 7.80-7.77 (m, 2H, H<sub>24</sub>/H<sub>26</sub>), 7.68-7.38 (m, 8H, H<sub>23</sub>/H<sub>27</sub>, H<sub>29</sub>/H<sub>31</sub>, H<sub>7</sub>, H<sub>30</sub>, H<sub>9</sub>/H<sub>13</sub>), 7.04 (d, 2H, *J* = 9.0 Hz, 39.13% (*E*), H<sub>10</sub>/H<sub>12</sub>), 7.00-6.96 (m, 4H, H<sub>9</sub>/H<sub>13</sub>, 60.86% (*Z*), H<sub>10</sub>/H<sub>12</sub>), 3.77, 3.76 (2s, 3H, 60.94% (*Z*), 39.06% (*E*), OCH<sub>3</sub>); Anal. Calc for C<sub>26</sub>H<sub>19</sub>BrN<sub>4</sub>O<sub>2</sub>S: C, 58.76; H, 3.60; N, 10.54; Found: C, 58.73; H, 3.57; N, 10.45.

### 3.4.13 | 5-((3-[4-Fluorophenyl]-1-phenyl-1*H*-pyrazol-4-yl)methylene)-2-(4-methoxyphenylimino) thiazolidin-4-one (THZP11)

Yield: 78%; mp >300°C; IR ( $\nu_{max}$  cm<sup>-1</sup>, KBr): 3024 (N—H lactam), 1713 (C=O lactam), 1643 (C=C), 1605 (C=N); <sup>1</sup>H NMR ( $\delta_{ppm}$ , 500 MHz, DMSO-*d*<sub>6</sub>):  $\delta$  8.70, 8.61 (2s, 1H, 40.0% (*E*), 60.0% (*Z*), H<sub>17</sub>), 7.99 (d, *J* = 8.2 Hz, 2H, 39.27% (*E*), H<sub>28</sub>/H<sub>32</sub>), 7.95 (d, *J* = 8.3 Hz, 2H, 60.73% (*Z*), H<sub>28</sub>/H<sub>32</sub>), 7.72-6.97 (m, 12H, H<sub>10</sub>/H<sub>12</sub>, H<sub>9</sub>/H<sub>13</sub>, H<sub>24</sub>/H<sub>26</sub>, H<sub>7</sub>, H<sub>30</sub>, H<sub>23</sub>/H<sub>27</sub>, H<sub>29</sub>/H<sub>31</sub>), 3.78, 3.77 (2s, 3H, 58.63% (*Z*), 41.43% (*E*), OCH<sub>3</sub>); Anal. Calc. For C<sub>26</sub>H<sub>19</sub>FN<sub>4</sub>O<sub>2</sub>S: C, 66.37; H, 4.07; N, 11.91; Found: C, 66.35; H, 4.01; N, 11.85.

### 3.4.14 | 5-((3-[4-Chlorophenyl]-1-phenyl-1*H*-pyrazol-4-yl)methylene)-2-(4-methoxyphenylimino) thiazolidin-4-one (THZP12)

Yield: 85%; mp >300°C; IR ( $\nu_{max}$  cm<sup>-1</sup>, KBr): 3072 (N—H lactam), 1713 (C=O lactam), 1643 (C=C), 1605 (C=N); <sup>1</sup>H NMR ( $\delta_{ppm}$ , 500 MHz, DMSO-*d*<sub>6</sub>):  $\delta$  8.72, 8.63 (2s, 1H, 41.0% (*E*), 59.0% (*Z*), H<sub>17</sub>), 7.99 (d, *J* = 8.5 Hz, 2H, 40.90% (*E*), H<sub>28</sub>/H<sub>32</sub>), 7.95 (d, *J* = 7.5 Hz, 2H, 59.09% (*Z*), H<sub>28</sub>/H<sub>32</sub>), 7.70-6.95 (m, 12H, H<sub>23</sub>/H<sub>27</sub>, H<sub>24</sub>/H<sub>26</sub>, H<sub>29</sub>/H<sub>31</sub>, H<sub>7</sub>, H<sub>30</sub>, H<sub>9</sub>/H<sub>13</sub>, H<sub>10</sub>/H<sub>12</sub>), 3.78, 3.71 (2s, 3H, 61.29% (*Z*), 38.71% (*E*), OCH<sub>3</sub>); Anal. Calc for C<sub>26</sub>H<sub>19</sub>ClN<sub>4</sub>O<sub>2</sub>S: C, 64.13; H, 3.93; N, 11.51; Found: C, 64.10; H, 3.90; N, 11.47.

### 3.4.15 | 5-([1,3-Diphenyl-1*H*-pyrazol-4-yl)methylene)-2-(4-methoxyphenylimino) thiazolidin-4-one (THZP13)

Yield: 79%; mp 293-295°C; IR ( $\nu_{max}$  cm<sup>-1</sup>, KBr): 3047 (N—H lactam), 1713 (C=O lactam), 1643 (C=C), 1605 (C=N); <sup>1</sup>H NMR ( $\delta_{ppm}$ , 500 MHz, DMSO-*d*<sub>6</sub>):  $\delta$  8.70, 8.62 (2s, 1H, 40.0% (*E*), 60.0% (*Z*), H<sub>17</sub>), 7.99 (d, *J* = 8.0 Hz, 2H, 41.06% (*E*), H<sub>28</sub>/H<sub>32</sub>), 7.96 (d, *J* = 8.0 Hz, 2H, 58.93% (*Z*), H<sub>28</sub>/H<sub>32</sub>), 7.71-7.52 (m, 9H, H<sub>23</sub>/H<sub>27</sub>, H<sub>9</sub>/H<sub>13</sub>, H<sub>29</sub>/H<sub>31</sub>,

H<sub>24</sub>/H<sub>26</sub>, H<sub>25</sub>), 7.46-7.38 (m, 2H, H<sub>7</sub>, H<sub>30</sub>), 7.06-6.98 (m, 4H, H<sub>9</sub>/H<sub>13</sub>, H<sub>10</sub>/H<sub>12</sub>), 3.78, 3.77 (2s, 3H, 59.71% (*Z*), 40.28% (*E*), OCH<sub>3</sub>); Anal. Calc for C<sub>26</sub>H<sub>20</sub>N<sub>4</sub>O<sub>2</sub>S: C, 69.01; H, 4.45; N, 12.38; Found: C, 68.98; H, 4.40; N, 12.31.

### 3.4.16 | 2-(4-Methoxyphenylimino)-5-((3-[4-nitrophenyl]-1-phenyl-1*H*-pyrazol-4-yl)methylene) thiazolidin-4-one (THZP14)

Yield: 83%; mp >300°C; IR ( $\nu_{max}$  cm<sup>-1</sup>, KBr): 3117 (N—H lactam), 1716 (C=O lactam), 1690 (C=C), 1605 (C=N); <sup>1</sup>H NMR ( $\delta_{ppm}$ , 500 MHz, DMSO-*d*<sub>6</sub>):  $\delta$  8.76, 8.68 (2s, 1H, 40.86% (*Z*), 59.14% (*E*), H<sub>17</sub>), 8.42 (d, *J* = 9.5 Hz, 1H, H<sub>24</sub>/H<sub>26</sub>), 8.02-7.93 (m, 4H, H<sub>28</sub>/H<sub>32</sub>, H<sub>23</sub>/H<sub>27</sub>), 7.71-7.36 (m, 6H, H<sub>9</sub>/H<sub>13</sub>, H<sub>29</sub>/H<sub>31</sub>, H<sub>7</sub>, H<sub>30</sub>), 7.01-6.95 (m, 4H, H<sub>9</sub>/H<sub>13</sub>, H<sub>10</sub>/H<sub>12</sub>), 3.77 (s, 3H, OCH<sub>3</sub>); Anal. Calc for C<sub>26</sub>H<sub>19</sub>N<sub>5</sub>O<sub>4</sub>S: C, 62.77; H, 3.85; N, 14.08; Found: C, 62.76; H, 3.86; N, 14.02.

## 3.5 | Enzyme inhibition assay

### 3.5.1 | Assay for $\alpha$ -amylase inhibition

The  $\alpha$ -amylase inhibition study was done using reported protocol with slight modifications.<sup>[62]</sup> Stock solutions for all the compounds were prepared in DMSO by dissolving 1 mg of compound in 1 mL of solvent. Six different concentrations (3.125, 6.25, 12.5, 25, 50, 100  $\mu$ g/mL) were used to evaluate the inhibition potential against  $\alpha$ -amylase from *A. oryzae*. All the solutions required for the inhibition studies were prepared according to already reported procedure.<sup>[62]</sup> The absorbances were measured at 650 nm using microplate reader.

### 3.5.2 | Assay for $\alpha$ -glucosidase inhibition

Chromogenic method with slight modification was used to evaluate the  $\alpha$ -glucosidase (obtained from *S. cerevisiae*) inhibitory activities.<sup>[63]</sup> Six different concentrations (3.125, 6.25, 12.5, 25, 50, 100  $\mu$ g/mL) were prepared for all the compounds. All the solutions required for the inhibition studies were prepared according to already reported procedure.<sup>[63]</sup> The blank solution was devoid of  $\alpha$ -glucosidase and the standard drug acarbose was used as positive control. Experiments were performed in triplicate and the absorbance was measured at 450 nm using microplate. The enzyme inhibitory rates of samples were calculated as follows:

$$\% \text{Inhibition} = (\text{Control} - \text{Sample}) / \text{Control} \times 100$$

### 3.6 | Computational studies

#### 3.6.1 | DFT studies

All calculations have been performed using Gaussian09<sup>[64]</sup> quantum-chemical package. The relative thermodynamic stability for (2Z,5Z) and (2E,5Z) isomer of both the compounds (**THZP1** and **THZP8**) was assessed using the energy of the optimized structures for both the isomers. The structure of all the compounds was optimized using B3LYP<sup>[46]</sup> exchange-correlation functional with 6-311G basis set.<sup>[65,66]</sup> The anisotropy of polarizability  $\Delta\alpha$  and its mean first order hyperpolarizability  $\langle\beta\rangle$  were calculated by the following equations<sup>[67]</sup> using the x, y, z components (Equations 1 and 2).

$$\Delta\alpha = \sqrt{\frac{(\alpha_{xx} - \alpha_{yy})^2 + (\alpha_{yy} - \alpha_{zz})^2 + (\alpha_{zz} - \alpha_{xx})^2}{2}} \quad (1)$$

$$\beta_{\text{tot}} = \left[ (\beta_{xxx} + \beta_{xyy} + \beta_{zzz})^2 + (\beta_{yyy} + \beta_{yzz} + \beta_{yxx})^2 + (\beta_{zzz} + \beta_{zxx} + \beta_{zyy})^2 \right]^{1/2}, \quad (2)$$

where  $\alpha_{xx}$ ,  $\alpha_{yy}$ , and  $\alpha_{zz}$  represents the components of polarizability and  $\beta_x$ ,  $\beta_y$ , and  $\beta_z$  are tensor components of hyperpolarizability.

#### 3.6.2 | Docking simulations

Marvin sketch was used for preparing an optimized 3D structure of both compound **THZP9** and **THZP14**. The protein data bank was assessed for the PDB structure of  $\alpha$ -amylase for *A. oryzae* (PDB ID: 7TAA) (<http://www.rcsb.org/pdb>). The protein was prepared by using UCSF Chimera 1.10<sup>[68]</sup> in which co-crystallized ligand and solvent molecules were removed to avoid interference in binding interactions. Missing side-chain gaps were filled using Dun Brack Rotamer library.<sup>[69]</sup> Gasteiger charges were calculated using AMBERf14SB and antechamber<sup>[70]</sup> and hydrogens were added. The Docking studies were performed using Auto Dock Vina 1.1.2.<sup>[71]</sup> Grid center with the following size center\_x = 40.1983719675, center\_y = 37.596211689, center\_z = 31.4482747318, size\_x = 21.9397670481, size\_y = 25.0, and size\_z = 20.2076584074 were placed on the active site. The results of docking studies were analyzed in discovery studio 2016 client.<sup>[61]</sup>

The protein sequence for Baker's yeast  $\alpha$ -glucosidase (MAL12 & MAL32) was retrieved from UniProt (<http://www.uniprot.org>). Homology model for *S. cerevisiae*  $\alpha$ -glucosidase was constructed using crystal structure of

isomaltase in complex with isomaltose of *S. cerevisiae* (strain ATCC 204508 / S288c) (PDB ID: 3AXH), which have 72% identical and 85% similar sequence with  $\alpha$ -glucosidase of *S. cerevisiae*. Swiss-Model was used for the sequence alignment and homology modelling,<sup>[72]</sup> which was further evaluated using PROCHECK.<sup>[73]</sup> Then, the most active compound **THZP14** was docked into the active site (Asp214, Glu276, Asp 349, and Arg439) of prepared model of *S. cerevisiae* using the Auto Dock Vina program.<sup>[71]</sup> Grid center was placed on the active site. The centers and sizes of the grid box were as follows: center\_x = -21.7738263108, center\_y = -5.92333172777, center\_z = -21.0706013836, size\_x = 20.7667725457, size\_y = 20.3967525101, and size\_z = 25.0. The discovery studio 2016 client and PyMol<sup>[74]</sup> were used for visualization of docking results.

## 4 | CONCLUSION

We have synthesized molecular hybrids based on thiazolidin-4-one and pyrazolyl pharmacophore (**THZP**) as new antidiabetic agents. Spectroscopic analyses (IR, <sup>1</sup>H NMR, MS) were done to confirm the structures of all the newly synthesized hybrids (**THZP**). The presence of two sets of signals in <sup>1</sup>H NMR of **3b** and one set of signal in **3a** revealed the existence of two configurational isomers (*E* and *Z*) in case of **3b**. Two sets of signals were come into view in <sup>1</sup>H NMR of **THZP8-THZP14** exhibited the presence of a configurational isomeric mixture of 2E,5Z (38.24%-41.58%) and 2Z,5Z isomers (58.42%-61.76%), which was further endorsed by DFT studies. DFT-based global chemical descriptors were calculated to describe the reactivity and to develop a relationship with biological activities. All the compounds (**THZP1-THZP14**) exhibit promising nonlinear optical properties (NLO). Further, the biological potential of all the synthesized compounds (**THZP1-THZP8**) was explored in terms of  $\alpha$ -amylase and  $\alpha$ -glucosidase inhibition studies. Compounds **THZP9** and **THZP14** showed remarkable inhibition of  $\alpha$ -amylase and  $\alpha$ -glucosidase with IC<sub>50</sub> 9.90 $\mu$ M and 4.84 $\mu$ M, respectively, as compared with standard drug acarbose (IC<sub>50</sub> 47.86 $\mu$ M for  $\alpha$ -amylase & 10.53 $\mu$ M for  $\alpha$ -glucosidase). Docking studies further supported the results of the activity.

## ACKNOWLEDGMENT

M.D. thanks the Haryana State Council of Science and Technology (HSCTC) for the award of research fellowship. The authors also thank SAIF PU for spectral data.

## ORCID

Parvin Kumar  <https://orcid.org/0000-0002-2635-6465>

## REFERENCES

- [1] N. Unwin, J. Shaw, P. Zimmet, K. Alberti, *Diabetic med* **2002**, *19*, 708.
- [2] A. Accurso, R. K. Bernstein, A. Dahlqvist, B. Draznin, R. D. Feinman, E. J. Fine, A. Gleed, D. B. Jacobs, G. Larson, R. H. Lustig, *Nutr metab* **2008**, *5*, 9.
- [3] T. Tuomi, N. Santoro, S. Caprio, M. Cai, J. Weng, L. Groop, *Lancet* **2014**, *383*, 1084.
- [4] Control, D.; Group, C. T. R. *NE J Med* **1993**, *329*, 977.
- [5] D. Daneman, *Diabetes care* **2001**, *24*, 801.
- [6] I. Mišur, K. Žarković, A. Barada, L. Batelja, Z. Miličević, Z. Turk, *Acta diabetol* **2004**, *41*, 158.
- [7] K. Sugimoto, M. Yasujima, S. Yagihashi, *Curr pharm des* **2008**, *14*, 953.
- [8] J. M. Forbes, M. E. Cooper, *Amino Acids* **2012**, *42*, 1185.
- [9] M. Lassila, K. K. Seah, T. J. Allen, V. Thallas, M. C. Thomas, R. Candido, W. C. Burns, J. M. Forbes, A. C. Calkin, M. E. Cooper, *J Am Soc Nephrol* **2004**, *15*, 2125.
- [10] Y. Sharma, S. Saxena, A. Mishra, A. Saxena, S. M. Natu, *J Ocul Biol Dis infor* **2012**, *5*, 63.
- [11] M. Chen, T. Curtis, A. Stitt, *Curr Med Chem* **2013**, *20*, 3234.
- [12] M. Peppia, S. A. Raptis, *Curr Diabetes Rev* **2008**, *4*, 92.
- [13] Z. Hegab, S. Gibbons, L. Neyses, M. A. Mamas, *World J cardiol* **2012**, *4*, 90.
- [14] N. Pantidos, A. Boath, V. Lund, S. Conner, G. McDougall, *J J Funct Foods* **2014**, *10*, 201.
- [15] B. W. Zhang, Y. Xing, C. Wen, X. X. Yu, W. L. Sun, Z. L. Xiu, Y. S. Dong, *Bioorg Med Chem lett* **2017**, *27*, 5065.
- [16] K. Han, Y. Li, Y. Zhang, Y. Teng, Y. Ma, M. Wang, R. Wang, W. Xu, Q. Yao, Y. Zhang, *Bioorg Med Chem lett* **2015**, *25*, 1471.
- [17] D. Semaan, J. Igoli, L. Young, E. Marrero, A. Gray, E. Rowan, *J Ethnopharmacol* **2017**, *203*, 39.
- [18] L. Han, C. Fang, R. Zhu, Q. Peng, D. Li, M. Wang, *Int J Biol Macromol* **2017**, *95*, 520.
- [19] J. Yan, G. Zhang, J. Pan, Y. Wang, *Int J Biol Macromol* **2014**, *64*, 213.
- [20] L. Zeng, G. Zhang, Y. Liao, D. Gong, *Food Funct* **2016**, *7*, 3953.
- [21] M. R. Bhosle, J. R. Mali, S. Pal, A. K. Srivastava, R. A. Mane, *Bioorg Med Chem lett* **2014**, *24*, 2651.
- [22] P. Kumar, M. Duhan, K. Kadyan, J. Sindhu, S. Kumar, H. Sharma, *Med Chem Comm* **2017**, *8*, 1468.
- [23] J. Dwivedi, K. Devi, Y. Asmat, S. Jain, S. Sharma, *J Saudi Chem Soc* **2016**, *20*, S16.
- [24] J. Sindhu, H. Singh, J. Khurana, C. Sharma, K. Aneja, *Chin Chem Lett* **2015**, *26*, 50.
- [25] D. D. Subhedar, M. H. Shaikh, M. A. Arkile, A. Yeware, D. Sarkar, B. B. Shingate, *Bioorg Med Chem lett* **2016**, *26*, 1704.
- [26] Y. Ali, M. S. Alam, H. Hamid, A. Husain, A. Dhulap, S. Bano, C. Kharbanda, *Bioorg Med Chem lett* **2017**, *27*, 1017.
- [27] M. F. Ansari, D. Idrees, M. I. Hassan, K. Ahmad, F. Avecilla, A. Azam, *Eur J Med Chem* **2018**, *144*, 544.
- [28] K. Liaras, M. Fesatidou, A. Geronikaki, *Molecules* **2018**, *23*, 685.
- [29] S. Jain, A. Kumar, D. Saini, *Exp Parasitol* **2018**, *185*, 107.
- [30] P. Balaji, D. Ranganayakulu, G. S. Reddy, *Asian J Pharm* **2017**, *3*, 9.
- [31] M. F. Shehry, M. M. Ghorab, S. Y. Abbas, E. A. Fayed, S. A. Shedid, Y. A. Ammar, *Eur J Med Chem* **2018**, *143*, 1463.
- [32] J. R. Badgujar, D. H. More, J. S. Meshram, *Indian J Microbiol* **2018**, *58*, 93.
- [33] H. Dai, S. Ge, J. Guo, M. Chen, Huang, J. Yang, S. Sun, Y. Ling, Y. Shi, *Eur J Med Chem* **2018**, *143*, 1066.
- [34] H. Liu, Z. L. Ren, W. Wang, J. X. Gong, M. J. Chu, Q. W. Ma, J. C. Wang, X. H. Lv, *Eur J Med Chem* **2018**, *157*, 81.
- [35] H. A. Elhady, R. El-Sayed, H. S. Al-nathali, *Chem Cent J* **2018**, *12*, 51.
- [36] M. J. Naim, O. Alam, M. J. Alam, M. Q. Hassan, N. Siddiqui, V. Naidu, M. I. Alam, *Bioorg Chem* **2018**, *76*, 98.
- [37] P. Kumar, R. Bhatia, R. Khanna, A. Dalal, D. Kumar, P. Surain, R. C. Kamboj, *J Sulfur Chem* **2017**, *38*, 585.
- [38] P. Kumar, K. Kadyan, M. Duhan, J. Sindhu, V. Singh, B. S. Saharan, *Chem Cent J* **2017**, *11*, 115.
- [39] A. Kumar, A. Chawla, S. Jain, P. Kumar, S. Kumar, *Med Chem Res* **2011**, *20*, 678.
- [40] S. Kumar, Meenakshi, S. Kumar, P. Kumar, *Med Chem Res* **2013**, *22*, 433.
- [41] P. Kumar, A. Kumar, J. Sindhu, S. Lal, *Drug Res.* **2018**, *69*, 159. <https://doi.org/10.1055/a-0652-5290>.
- [42] P. Kumar, S. Kumar, K. Husain, A. Kumar, *Chin Chem Lett* **2011**, *22*, 37.
- [43] S. Ramsh, N. Smorygo, E. Khrabrova, A. Ginak, *Chem Heterocycl Com* **1986**, *22*, 447.
- [44] R. Ottana, R. Maccari, M. L. Barreca, G. Bruno, A. Rotondo, A. Rossi, G. Chiricosta, R. D. Paola, L. Sautebin, S. Cuzzocrea, *Bioorg Med Chem* **2005**, *13*, 4243.
- [45] E. Runge, E. K. Gross, *Phys Rev Lett* **1984**, *52*, 997.
- [46] P. Stephens, F. Devlin, C. Chabalowski, M. Frisch, *J J Phys Chem A* **1994**, *98*, 11623.
- [47] D. M. Gil, M. D. Lestard, O. E. Hernández, J. Duque, E. Reguera, *Spectrochim Acta A Mol Biomol Spectros* **2015**, *145*, 553.
- [48] R. Parthasarathi, V. Subramanian, D. R. Roy, P. Chattaraj, *Bioorg Med Chem* **2004**, *12*, 5533.
- [49] F. De Proft, P. Geerlings, *Chem Rev* **2001**, *101*, 1451.
- [50] Chattaraj, P. K.; Roy, D. R. *Chem Rev* **2007**, *107*, 9, 46.
- [51] J. L. Reed, *J Phys Chem A* **1997**, *101*, 7396.
- [52] Pauling, L. The Nature of the Chemical Bond Cornell university press Ithaca, NY, **1960**.
- [53] R. G. Parr, W. Yang, *J Am Chem Soc* **1984**, *106*, 4049.
- [54] T. Koopmans, *Physica A* **1933**, *1*, 104.
- [55] L. Ferreira, R. D. Santos, G. Oliva, A. Andricopulo, *Molecules* **2015**, *20*, 13384.
- [56] S. J. Y. Macalino, V. Gosu, S. Hong, S. Choi, *Arch Pharm Res* **2015**, *38*, 1686.
- [57] B. Svensson, *Plant Mol Biol* **1994**, *25*, 141.
- [58] R. Laskowski, M. MacArthur, D. Moss, J. Thornton, *J Appl Crystallogr* **1993**, *24*, 946.
- [59] S. B. Ferreira, A. C. Soderro, M. F. Cardoso, E. S. Lima, C. R. Kaiser, F. P. Silva, V. F. Ferreira, *J Med Chem* **2010**, *53*, 2364.
- [60] Morris, G.; Goodshell, D.; Huey, R.; Hart, W.; Halliday, R.; Belew, R.; Olson, A. Autodock (version 3.05), Molecular Graphics Laboratory, Department of Molecular Biology The Scripps Research Institutes, in, La Jolla, CA, USA, **1999**.
- [61] Visualizer, D. S. version **2016** 17.2.0.16349. Accelrys Software Inc, in.

- [62] N. Rani, S. K. Sharma, N. Vasudeva, *Evid Based Complement Alternat Med* **2012**, 2012, 1. <https://doi.org/10.1155/2012/715912>.
- [63] F. M. Afrapoli, B. Asghari, S. Saeidnia, Y. Ajani, M. Mirjani, M. Malmir, R. D. Bazaz, A. Hadjiakhoondi, P. Salehi, M. Hamburger, *DARU J Pharm Sci* **2012**, 20, 37.
- [64] M. Frisch, G. Trucks, H. Schlegel, G. Scuseria, M. Robb, J. Cheeseman, *GAUSSIAN09. Revision E*, Vol. 01, Gaussian Inc., Wallingford, CT, USA **2009**.
- [65] A. D. Becke, *J Chem phys* **1992**, 96, 2155.
- [66] C. Lee, W. Yang, R. G. Parr, *Phys Rev B Condens Matter* **1988**, 37, 785.
- [67] D. Avci, *Spectrochim Acta A* **2011**, 82, 37.
- [68] E. F. Pettersen, T. D. Goddard, C. C. Huang, G. S. Couch, D. M. Greenblatt, E. C. Meng, T. E. Ferrin, *J Comput Chem* **2004**, 25, 1605.
- [69] Dunbrack, R. L. *Curr Opin Struc Biol* **2002**, 12, 431, Rotamer Libraries in the 21st Century, 440.
- [70] J. Wang, W. Wang, P. A. Kollman, D. Case, *A. J Mol Graph model* **2006**, 25, 247.
- [71] O. Trott, A. Olson, *J. J Comput Chem* **2010**, 31, 455.
- [72] Waterhouse, A.; Bertoni, M.; Bienert, S.; Studer, G.; Tauriello, G.; Gumienny, R.; Heer, F. T.; Beer, T. A. P.; Rempfer, C.; Bordoli, L. *Nucleic Acids Res* **2018**, 46(W1), W296. <https://doi.org/10.1093/nar/gky427>
- [73] DeLano, W. The PyMOL Molecular Graphics System, Version 1.1. Schrödinger LLC. **2002**. Google Scholar 2014.
- [74] R. A. Laskowski, J. A. C. Rullmann, M. W. MacArthur, R. Kaptein, J. M. Thornton, *J Biomol NMR* **1996**, 8, 477.

## SUPPORTING INFORMATION

Additional supporting information may be found online in the Supporting Information section at the end of this article.

**How to cite this article:** Kumar P, Duhan M, Sindhu J, Kadyan K, Saini S, Panihar N. Thiazolidine-4-one clubbed pyrazoles hybrids: Potent  $\alpha$ -amylase and  $\alpha$ -glucosidase inhibitors with NLO properties. *J Heterocycl Chem*. 2019;1–15. <https://doi.org/10.1002/jhet.3882>